Falkland Islands Fisheries Department

Loligo Stock Assessment, First Season 2014

Andreas Winter

May 2014

Index

Summary 3
Introduction 3
Methods 4
Stock assessment 9
  Data 9
  Group arrivals / depletion criteria 11
  Depletion analyses 13
    North 13
    South 14
  Escapement biomass 16
  Immigration 17
Evaluation of season extension 18
References 20
Appendix 23
  Prior estimates and CV 23
  Depletion model estimates and CV 24
  Sea wind patterns 28

Summary

1) The first season *Loligo* fishery of 2014 was open for the scheduled 57 days from February 24th to April 21st, with one vessel taking the flex option of two days' later start and finish. This season marked a scheduling change as the fishery was extended one week longer into April than previously, to be offset by starting second season one week later.
2) 28,119 tonnes of *Loligo* catch were reported in the commercial fishery; the 3rd-highest first season total since 2005. In the Loligo Box 61.3% of *Loligo* catch and 49.9% of effort were taken north of 52º S; 38.7% of *Loligo* catch and 50.1% of effort were taken south of 52º S.
3) Sub-areas north and south of 52º S were depletion-modelled separately. In the north sub-area, three in-season depletion periods were inferred to have started on February 24th, March 22nd, and April 13th. In the south sub-area, four in-season depletion periods were inferred to have started on February 27th, March 22nd, April 2nd, and April 12th.
4) Approximately 26,750 tonnes of *Loligo* (95% confidence interval: [10,398 to 46,512] tonnes) were estimated to have migrated into the Loligo Box during first season 2014, representing 46% of the *Loligo* biomass in the fishing zone.
5) The final total estimate for *Loligo* remaining in the Loligo Box at the end of first season 2014 was:
   Maximum likelihood of 30,500 tonnes, with a 95% confidence interval of [24,059 to 49,207] tonnes.
   The risk of *Loligo* escapement biomass at the end of the season being less than 10,000 tonnes was estimated at effectively zero.
6) The one-week extension yielded catches better than the average of the rest of the season, with in-season depletions having started just 1-2 days before the extension. Observer data measures showed no strong impact on the biological status of the *Loligo* stock over the course of the extension.

Introduction

The first season of the 2014 *Loligo* fishery (*Doryteuthis gahi* – Patagonian squid) started on February 24th with 15 vessels participating. One vessel took the flex rule option and started the season two days later on February 26th. The season ended by directed closure on April 21st (and two days later for the late-starting vessel). This season marked a change in scheduling with a one-week extension allocated in April, to be offset by postponing the start of second season by one week from July 15th to July 22nd. The change was implemented following consultation with fishing masters and retrospective analysis of potential outcomes for *Loligo* abundance and maturity distributions. The objective of the change is to equalize effort on the two annual *Loligo* cohorts and improve yield in the fishery without adversely affecting the sustainability of the *Loligo* population (Fisheries Committee, 2013). Total reported *Loligo* catch by C-licensed vessels in the 2014 first season was 28,119 tonnes; the 3rd-highest first season (since 2005) after 2012 (34,767 t) and 2010 (28,754 t), and the 4th-highest in catch per vessel day at 28119/872 = 32.25 t, after 2012 (45.15 t), 2005 (42.72 t), and 2010 (37.59 t) (Table 1).

As in previous seasons, the *Loligo* stock assessment was conducted with depletion time-series models (Agnew et al., 1998; Roa-Ureta and Arkhipkin, 2007;

Arkhipkin et al., 2008). Because *Loligo* has an annual life cycle (Patterson, 1988; Arkhipkin et al., 2013), stock cannot be derived from a standing biomass carried over from prior years (Rosenberg et al., 1990). The depletion model instead calculates an estimate of population abundance over time by evaluating what levels of abundance and catchability must be extant to sustain the observed rate of catch. Depletion modelling is used both in-season and for the post-season summary, with the objective of maintaining an escapement biomass of 10,000 tonnes *Loligo* at the end of each season as a conservation threshold (Agnew et al., 2002; Barton, 2002).

Table 1. *Loligo* season catch comparisons since 2004. Days: total calendar days open to licensed *Loligo* fishing including (since 1st season 2013) optional extension days; V-Days: aggregate number of licensed *Loligo* fishing days reported by all vessels for the season.

	Season 1			Season 2		
	Catch (t)	Days	V-Days	Catch (t)	Days	V-Days
2004				17,559	78	1271
2005	24,605	45	576	29,659	78	1210
2006	19,056	50	704	23,238	53	883
2007	17,229	50	680	24,171	63	1063
2008	24,752	51	780	26,996	78	1189
2009	12,764	50	773	17,836	59	923
2010	28,754	50	765	36,993	78	1169
2011	15,271	50	771	18,725	70	1099
2012	34,767	51	770	35,026	78	1095
2013	19,908	53	782	19,614	78	1195
2014	28,119	59	872			

Methods

The depletion model formulated for the Falkland Islands *Loligo* stock is based on the equivalence:

$$C_{day} = q \times E_{day} \times N_{day} \times e^{-M/2} \quad \textbf{(1)}$$

where q is the catchability coefficient, M is natural mortality (considered constant at 0.0133 day^{-1}; Roa-Ureta and Arkhipkin, 2007), and C_{day}, E_{day}, N_{day} are catch (numbers of *Loligo*), fishing effort (numbers of vessels), and abundance (numbers of *Loligo*) per day. In its basic form (DeLury, 1947) the depletion model assumes a closed population in a fixed area for the duration of the assessment. However, the assumption of a closed population is imperfectly met in the Falkland Islands fishery, where stock analyses have often shown that *Loligo* groups arrive in successive waves after the start of the season (Roa-Ureta, 2012; Winter and Arkhipkin, 2012). Arrivals of successive groups are inferred from discontinuities in the catch data. Fishing on a single, closed cohort would be expected to yield gradually decreasing CPUE, but gradually increasing average individual sizes, as the squid grow. When instead these data change suddenly, or in contrast to expectation, the immigration of a new group to the population is indicated.

In the event of a new group arrival, the depletion calculation must be modified to account for this influx. This was done using a simultaneous algorithm (Roa-Ureta, 2012) that adds new arrivals on top of the stock previously present, and posits a common catchability coefficient for the entire depletion time-series. If two depletions are included in the same model (i.e., the stock present from the start plus a new group arrival), then:

$$C_{day} = q \times E_{day} \times (N1_{day} + (N2_{day} \times i2|_{0}^{1})) \times e^{-M/2} \quad \textbf{(2)}$$

where i2 is a dummy variable taking the values 0 or 1 if 'day' is before or after the start day of the second depletion. For more than two depletions, $N3_{day}$, i3, $N4_{day}$, i4, etc., would be included following the same pattern.

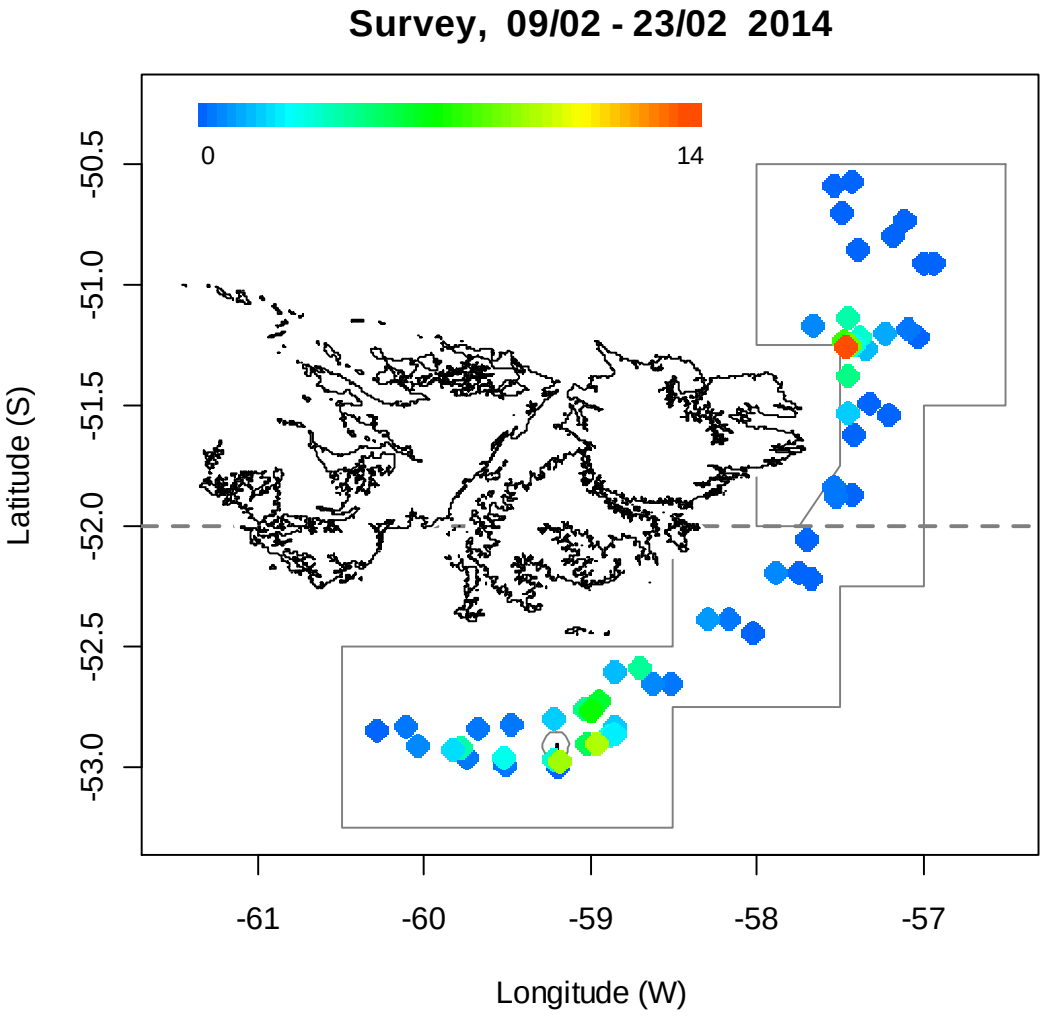

Figure 1. Spatial distribution of *Loligo* 1st-season pre-season survey catches, colour-scaled to catch weight (maximum = 14 tonnes). Sixty catches are represented. The 'Loligo Box' fishing zone, as well as the 52 ºS parallel delineating the boundary between north and south assessment sub-areas, are shown in gray.

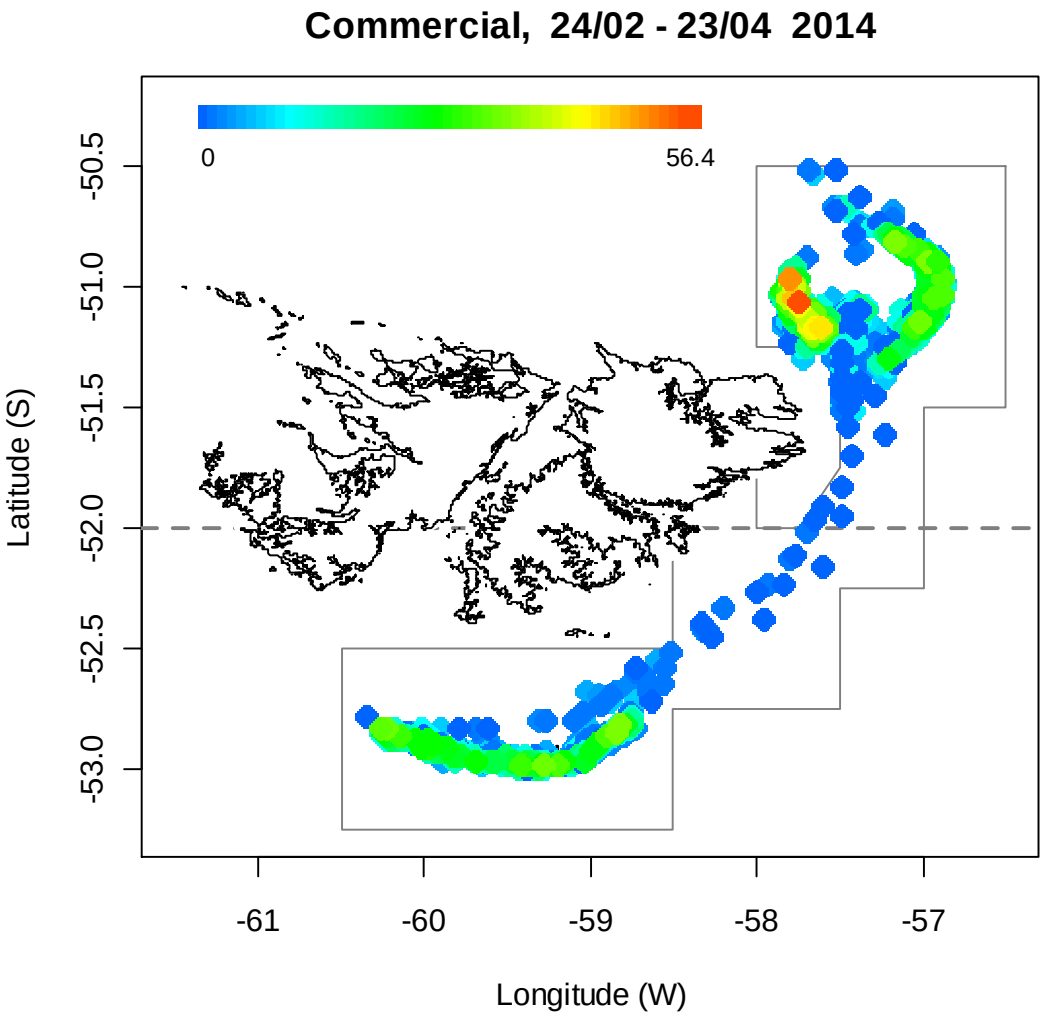

Figure 2. Spatial distribution of *Loligo* 1st-season commercial catches, colour-scaled to catch weight (maximum = 56.4 tonnes). 2820 catches were taken during the season. The 'Loligo Box' fishing zone, as well as the 52 ºS parallel delineating the boundary between north and south assessment sub-areas, are shown in gray.

The *Loligo* stock assessment was calculated in a Bayesian framework (Punt and Hilborn, 1997), whereby results of the season depletion model are conditioned by prior information on the stock; in this case the information from the pre-season survey. The season depletion likelihood function was calculated as the difference between actual catch numbers reported and catch numbers predicted from the model (equation **2**), statistically corrected by a factor relating to the number of days of the depletion period (Roa-Ureta, 2012):

$$((n\text{Days} - 2)/2) \times \log\left(\sum_{days}\left(\log(\text{predicted C}_{\text{day}}) - \log(\text{actual C}_{\text{day}})\right)^2\right) \qquad \textbf{(3)}$$

The survey prior likelihood function was calculated as the normal distribution of the difference between catchability (q) derived from the survey abundance estimate, and catchability derived from the season depletion model:

$$\frac{1}{\sqrt{2\pi \cdot \mathrm{SD}_{\mathrm{q\,survey}}{}^2}} \times \exp\left(-\frac{\left(\mathrm{q}_{\mathrm{model}} - \mathrm{q}_{\mathrm{survey}}\right)^2}{2 \cdot \mathrm{SD}_{\mathrm{q\,survey}}{}^2} \right) \quad \textbf{(4)}$$

Catchability, rather than abundance N, was used for calculating the survey prior likelihood because catchability informs the entire season time series; whereas N from the survey only informs the first season depletion period – subsequent immigrations and depletions are independent of the abundance that was present during the survey.

Bayesian optimization of the depletion was calculated by jointly minimizing equations **3** and **4**, using the Nelder-Mead algorithm in R programming package 'optimx' (Nash and Varadhan, 2011). Relative weights in the joint optimization were assigned to equations **3** and **4** as the converse of their coefficients of variation (CV), i.e., the CV of the prior became the weight of the depletion model and the CV of the depletion model became the weight of the prior. Calculations of the CVs are described in the Appendix.

With C_{day}, E_{day} and M being fixed parameters, the optimization of equation **2** using **3** and **4** produces estimates of q and N1, N2, …, etc. Numbers of *Loligo* on the final day (or any other day) of a time series are then calculated as the numbers N of the depletion start days discounted for natural mortality during the intervening period, and subtracting cumulative catch also discounted for natural mortality (CNMD). Taking for example a two-depletion period:

$$\begin{aligned} N_{\text{final day}} = {} & N1_{\text{start day 1}} \times e^{-M\,(\text{final day} - \text{start day 1})} \\ & + N2_{\text{start day 2}} \times e^{-M\,(\text{final day} - \text{start day 2})} \\ & - CNMD_{\text{final day}} \end{aligned} \quad \textbf{(5)}$$

where

$$\begin{aligned} CNMD_{\text{day 1}} &= 0 \\ CNMD_{\text{day x}} &= CNMD_{\text{day x-1}} \times e^{-M} + C_{\text{day x-1}} \times e^{-M/2} \end{aligned} \quad \textbf{(6)}$$

$N_{\text{final day}}$ is then multiplied by the average individual weight of *Loligo* on the final day to give biomass. Daily average individual weight is obtained from length / weight conversion of mantle lengths measured in-season by observers, and also derived from in-season commercial data as the proportion of product weight that vessels reported per market size category. Observer mantle lengths are scientifically precise, but restricted to 1-2 vessels at any one time that may or may not be representative of the entire fleet. Commercially proportioned mantle lengths are relatively imprecise, but cover the entire fishing fleet. Therefore, both sources of data are used. Daily average individual weights are calculated by averaging observer size samples and commercial size categories where observer data are available, otherwise only commercial size categories.

Distributions of the likelihood estimates from joint optimization (i.e., measures of their statistical uncertainty) were computed using a Markov Chain Monte Carlo (MCMC) (Gamerman and Lopes, 2006), a method that is commonly employed for fisheries assessments (Magnusson et al., 2013). MCMC is an iterative process which generates random stepwise changes to the proposed outcome of a model (in this case, the N and q of *Loligo*) and at each step, accepts or nullifies the change with a probability equivalent to how well the change fits the model parameters compared

to the previous step. The resulting sequence of accepted or nullified changes (i.e., the 'chain') approximates the likelihood distribution of the model outcome. The MCMC of the depletion models were run for 100,000 iterations; the first 1000 iterations were discarded as burn-in sections (initial phases over which the algorithm stabilizes); and the chains were thinned by a factor equivalent to the maximum of either 5 or the inverse of the acceptance rate (e.g., if the acceptance rate was 12.5%, then every 8th (0.125^{-1}) iteration was retained) to reduce serial correlation. For each model three chains were run; one chain initiated with the parameter values obtained from the joint optimization of equations **3** and **4**, one chain initiated with these parameters ×2, and one chain initiated with these parameters ×¼. Convergence of the three chains was accepted if the variance among chains was less than 10% higher than the variance within chains (Brooks and Gelman, 1998). When convergence was satisfied the three chains were combined as one final set. Equations **5**, **6**, and the multiplication by average individual weight were applied to CNMD and each iteration of N values in the final set, and the biomass outcomes from these calculations represent the distribution of the estimate. Maximum likelihood of biomass on each day was defined as the peak of the histogram of MCMC outcomes at 500-tonne intervals.

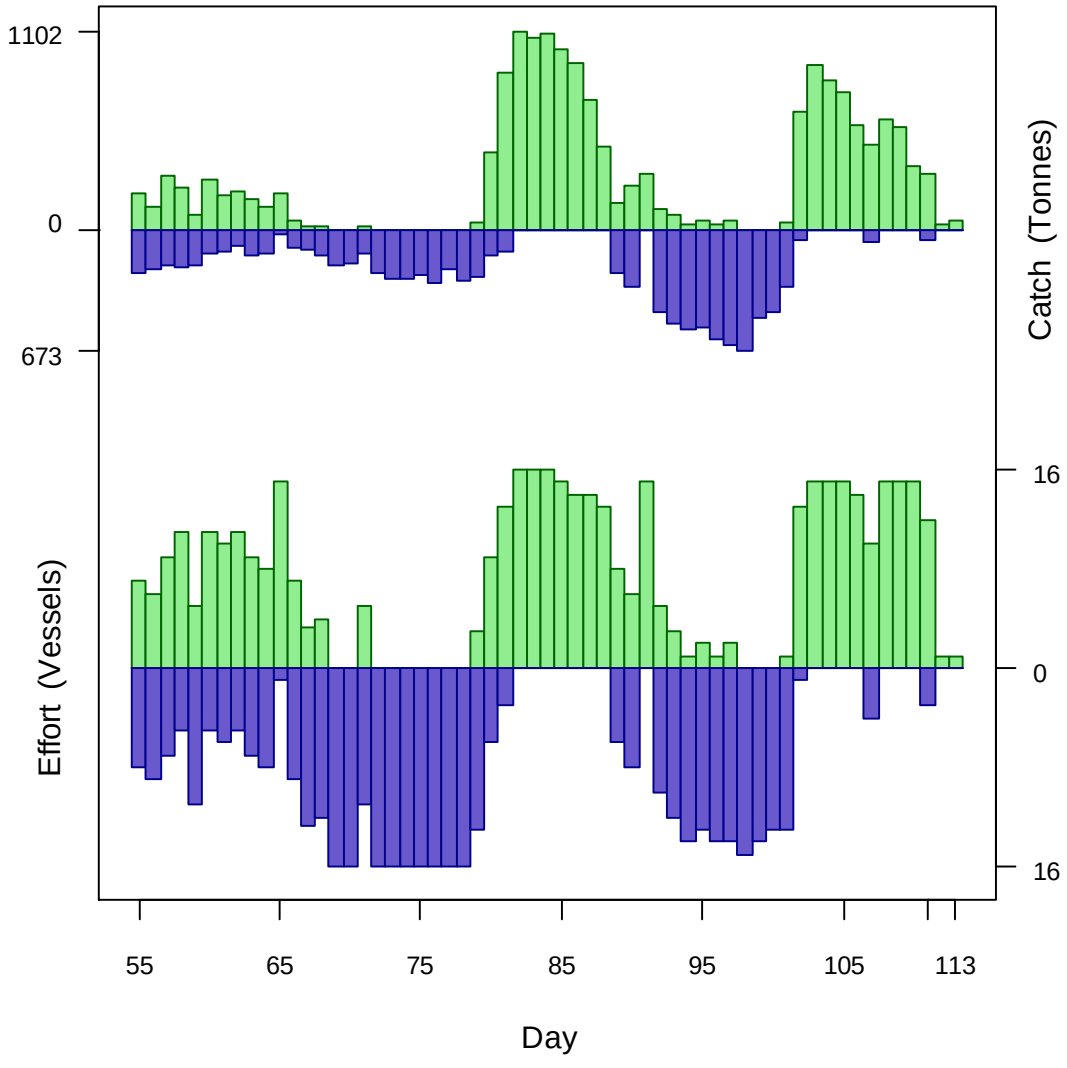

Figure 3 [previous page]. Daily total *Loligo* catch and effort distribution by assessment sub-area north (green) and south (purple) of 52º S parallel in *Loligo* 1st season 2014. The season was open from February 24th (chronological day 55) to April 21st (day 111) with one vessel on flex option to April 23rd (day 113). As many as 16 vessels fished per day north of 52º S; as many as 16 vessels fished per day south of 52º S. As much as 1102 tonnes *Loligo* was caught per day north of 52º S; as much as 673 tonnes *Loligo* was caught per day south of 52º S.

Stock assessment

Data

Pre-season survey catches and in-season commercial catches both showed a pattern of segregation with one zone of high concentration in the north and one in the south (Figures 1 and 2). In-season, 76.1% of total *Loligo* catch was taken in just 6 grids (trawl-end positions): in the north XNAN (31.4%), XMAP (6.7%) and XNAQ (6.2%); in the south XVAK (14.0%), XVAH (10.3%) and XVAJ (7.5%). The same six grids accounted for 64.9% of effort. Given the high level of segregation, sub-areas north and south of 52° S were depletion-modelled separately.

A total of 872 vessel-days were fished during the season, with a median of 15 vessels per day (Figure 3). These vessels reported daily catch totals to the FIFD and electronic logbook data that included trawl times, positions, and product weight by market size categories. Two FIFD observers were deployed on three vessels in the fishery for a total of 54 observer-days. Throughout the 59 days of the season, 6 days had no observer covering, 52 days had 1 observer covering, and 1 day had two observers covering. Each observer sampled an average of 414 *Loligo* daily, and reported their maturity stages, sex, and lengths to 0.5 cm. The length-weight relationship for converting both observer and commercially proportioned length data was taken from the pre-season survey (Winter and Jürgens, 2014):

$$\text{weight (kg)} = 0.170 \times \textit{length}\,(cm)^{2.251} / 1000 \qquad \textbf{(7)}$$

The season started relatively slowly, but catches in the north on March 23rd (day 82) set a single-day record for the *Loligo* fishery (A. Arkhipkin, FIFD, pers. comm.), with catches on the subsequent three days nearly equally high (Figure 3). The days leading up to these record catches were characterized by alternating westerly and northerly winds (Appendix Figure A3), which are known to correlate with increased immigration and aggregation of *Loligo* squid.

This season was further noted for its high incidence of medusae (jellyfish) in catches (Jones, 2014a, b; Lee, 2014; Figure 4). To quantify the incidence, discard records were reviewed from all previous 1st seasons that had used electronic logbooks. While medusae may be difficult to report accurately, comparisons show a strong increase over the past four years with medusae bycatches in 2014 being on average several times higher than in any preceding year (Figure 5). Jellyfish populations have been found in various regions to undergo large fluctuations, but recent analyses suggest increasing abundances in a majority of large marine ecosystems, including the Patagonian Shelf (Brotz et al., 2012).

Figure 4 [next page]. Video frame from a commercial trawl during 1st season showing large quantities of medusae emptying from the net along with *Loligo* catch. Video provided courtesy of the F/V *Venturer*.

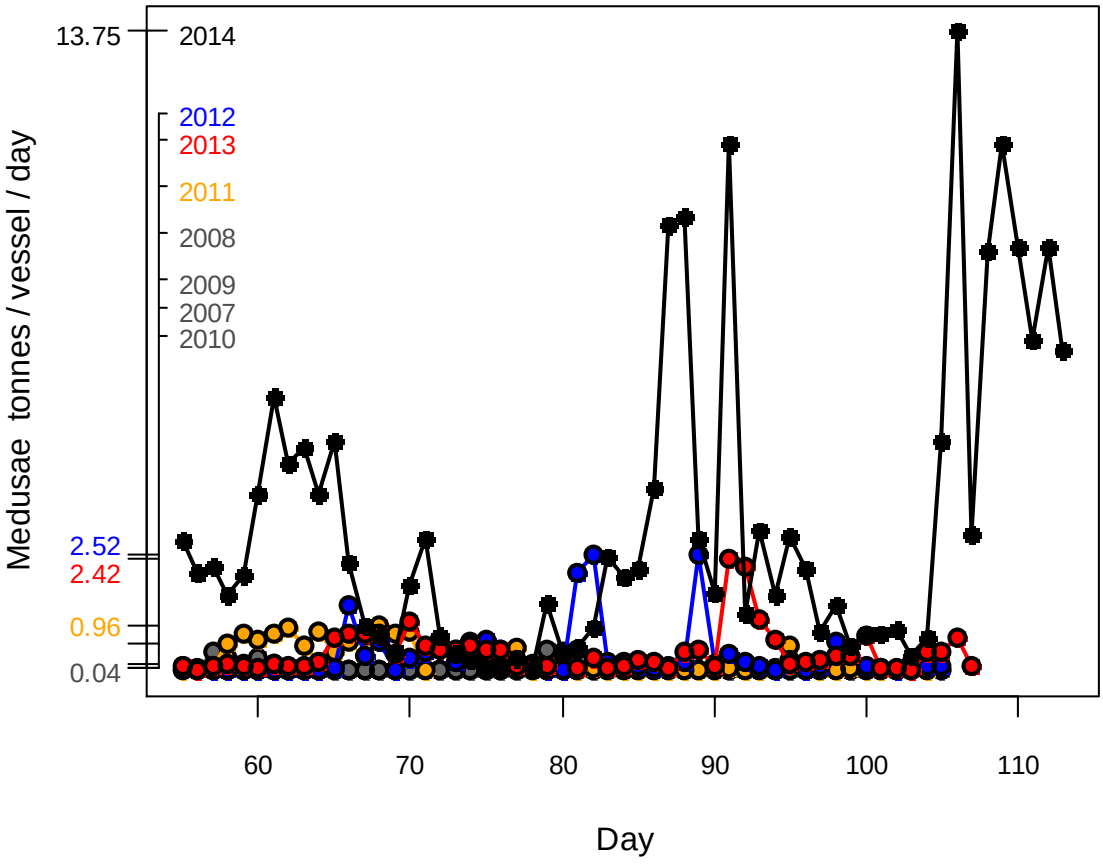

Figure 5. Medusae daily catches (tonnes / vessel / day) during *Loligo* 1st seasons 2007 – 2014. The Y-axis is marked at the maximum of each season.

Group arrivals / depletion criteria

Start and end days of depletions - following arrivals of new *Loligo* groups - were judged primarily with reference to daily changes in CPUE, with additional information from sex proportions, maturity, and average individual *Loligo* sizes. CPUE was calculated as metric tonnes of *Loligo* caught per vessel per day. Days were used rather than trawl hours as the basic unit of effort. Commercial vessels do not trawl standardized duration hours, but rather durations that best suit their daily processing requirements. An effort index of days is therefore more consistent.

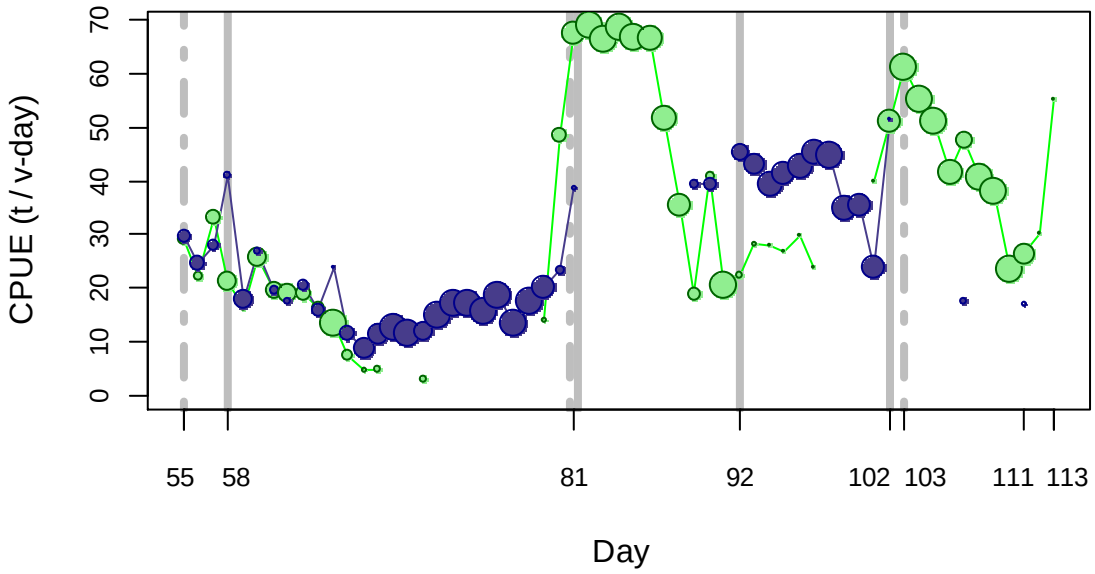

Figure 6. CPUE in metric tonnes per vessel per day, by assessment sub-area north (green) and south (purple) of the 52º S parallel. Circle sizes are proportioned to the numbers of vessel fishing. Data from consecutive days are joined by line segments. Broken gray bars indicate days 55, 81 and 103, identified as the start of in-season depletions north. Solid gray bars indicate days 58, 81, 92 and 102, identified as the start of in-season depletions south.

Three days in the north and four days in the south were identified that most plausibly represented the onset of separate depletions.

- The first in-season depletion north was identified on day 55 (February 24th - the start of the commercial season), after which a generally declining trend in CPUE was observed until day 71 (March 12th) (Figure 6).
- The second depletion north was identified on day 81 (March 22nd) with a strong CPUE peak culminating over two days (Figure 6), and accompanied by a local maximum in average commercial size category weights (Figure 7).
- The third depletion north was identified on day 103 (April 13th) with a CPUE peak subsequently declining until the end of the season (Figure 6), and local maxima in average weights and proportion of females in observer samples (Figure 7).
- The first in-season depletion south was identified on day 58 (February 27th) with a CPUE peak that was the highest for the next three weeks (Figure 6), and the start of an increasing trend in average male maturity (Figure 7).

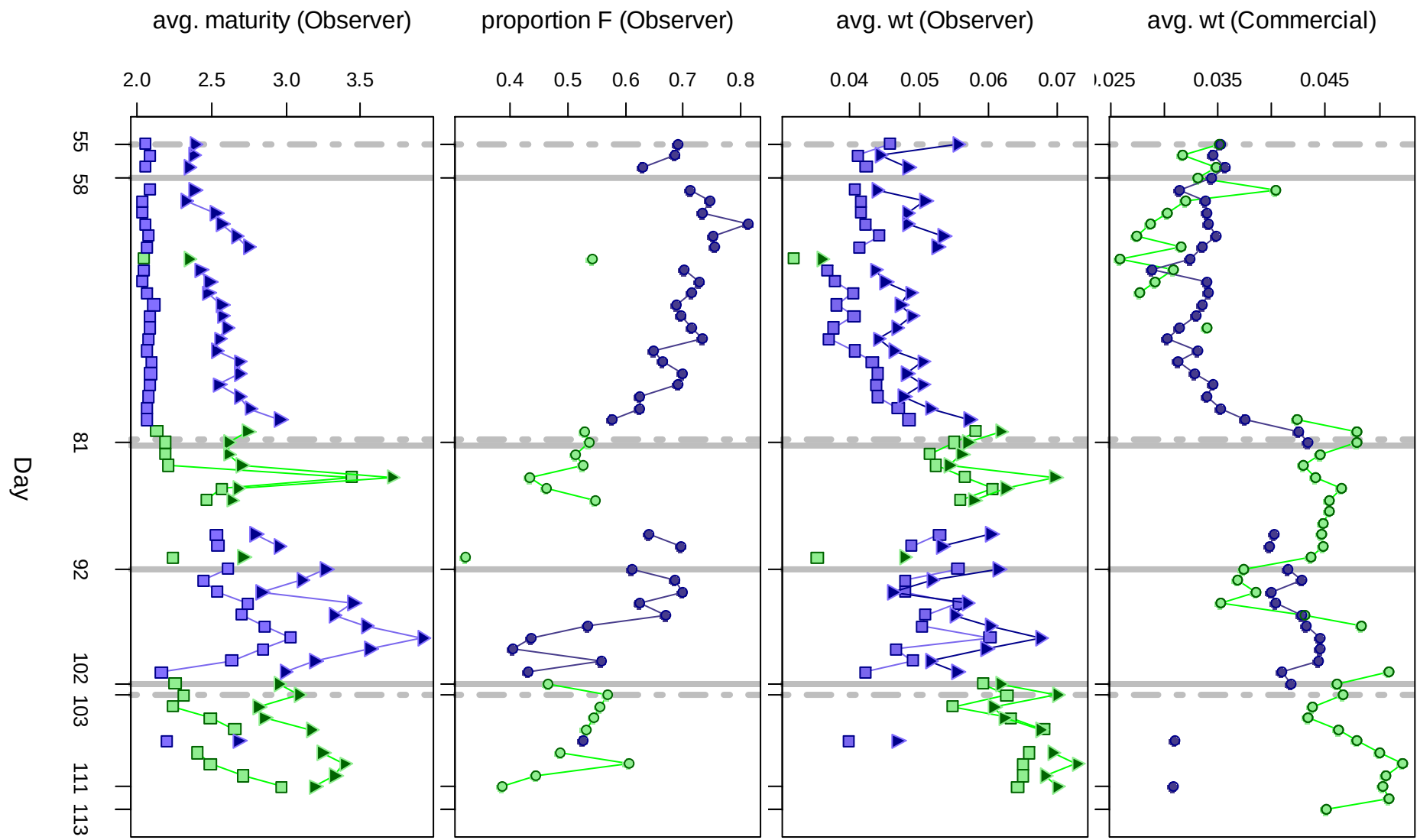
avg. maturity (Observer)
proportion F (Observer)
avg. wt (Observer)
avg. wt (Commercial)
2.0
2.5
3.0
3.5
0.4
0.5
0.6
0.7
0.8
0.04
0.05
0.06
0.07
.025
0.035
0.045
55
58
81
92
102
103
111
113
Day

Figure 7 [previous page]. Top graph: Average individual *Loligo* weights (kg) per day from commercial size categories. 2nd graph: Average individual *Loligo* weights (kg) by sex per day from observer sampling. 3rd graph: Proportions of female *Loligo* per day from observer sampling. Bottom graph: avg. maturity value by sex per day from observer sampling. In all graphs – Males: triangles, females: squares, unsexed: circles. North sub-area: green, south sub-area: purple. Data from consecutive days are joined by line segments. Broken gray bars indicate days 55, 81 and 103, identified as the start of in-season depletions north. Solid gray bars indicate days 58, 81, 92 and 102, identified as the start of in-season depletions south.

- The second depletion south was identified on day 81 (March 22nd) with a peak in CPUE (Figure 6) and a local maximum in average commercial size category weights (Figure 7).
- The third depletion south was identified on day 92 (April 2nd) with the highest level of CPUE south since the start of the season (Figure 6) and some indication of a local maximum in average weights from observer samples (Figure 7).
- The fourth depletion south was identified on day 102 (April 12th) with an increase in CPUE to its highest level of the season (Figure 6).

Depletion analyses
North

In the north sub-area, Bayesian optimization on catchability (q) resulted in a posterior (max. likelihood $q_N = 2.95 \times 10^{-3}$; Figure 8, left) that was closer to the pre-season prior ($_{prior}q_N = 2.84 \times 10^{-3}$; Figure 8, left, and equation **A3-N**) than to the in-season depletion ($_{depletion}q_N = 4.75 \times 10^{-3}$; Figure 8, left, and **A5-N**). In-season depletion had higher weight than the prior in the Bayesian optimization (0.558 to 0.278; **A4-N** and **A8-N**), but was relatively unselective for q.

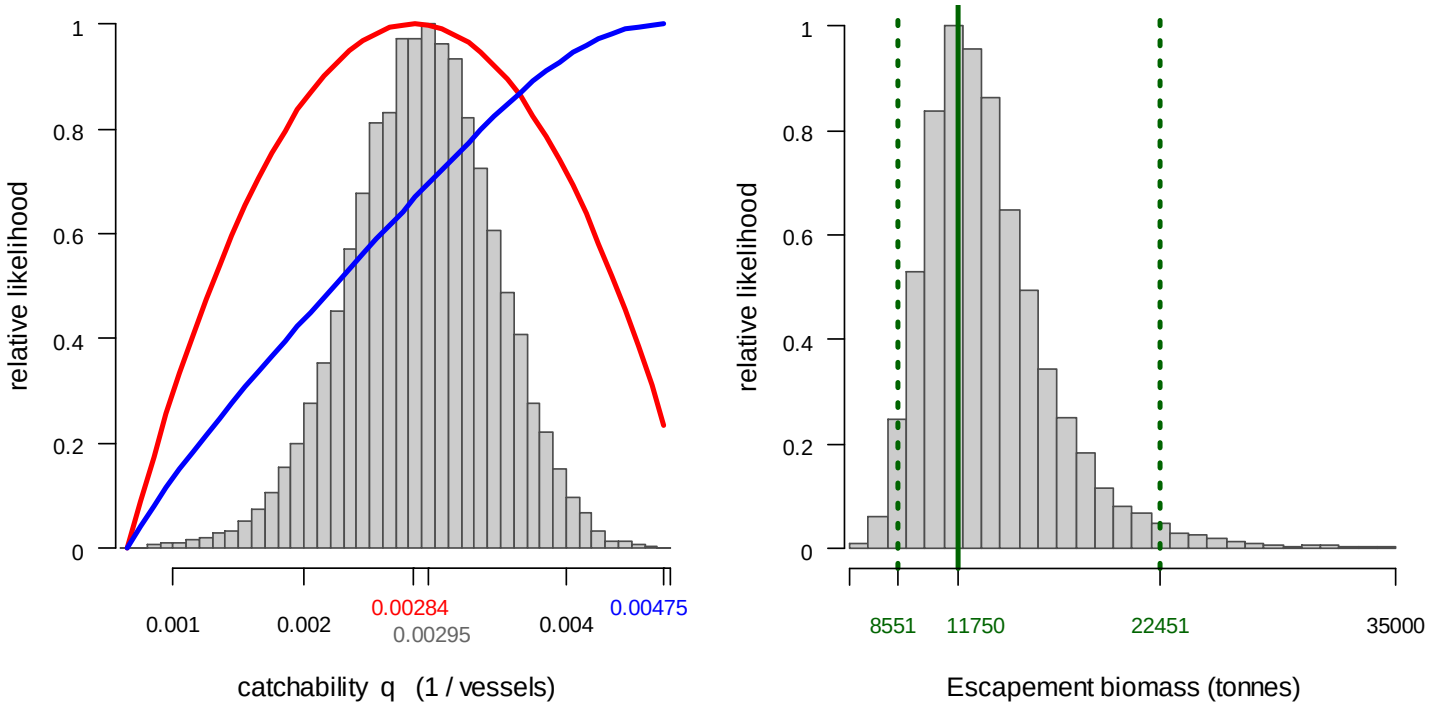

Figure 8 [previous page]. North sub-area. Left: Likelihood distributions for *Loligo* catchability. Red line: prior model (pre-season survey data), blue line: in-season depletion model, gray bars: combined Bayesian model. Right: Likelihood distribution (gray bars) of escapement biomass, from Bayesian posterior and average individual *Loligo* weight at the end of the season. Green lines: maximum likelihood and 95% confidence interval. Note the correspondence to Figure 9.

The MCMC distribution of the posterior multiplied by average individual *Loligo* weight on the final day of the season (45.1 g; Figure A2-N), gave the likelihood distribution of *Loligo* final-day biomass shown in Figure 8, right, with maximum likelihood and 95% confidence interval of:

$$B_{N\ day\ 113} = 11{,}750\ t \sim 95\%\ CI\ [8{,}551 - 22{,}451]\ t \quad \textbf{(8)}$$

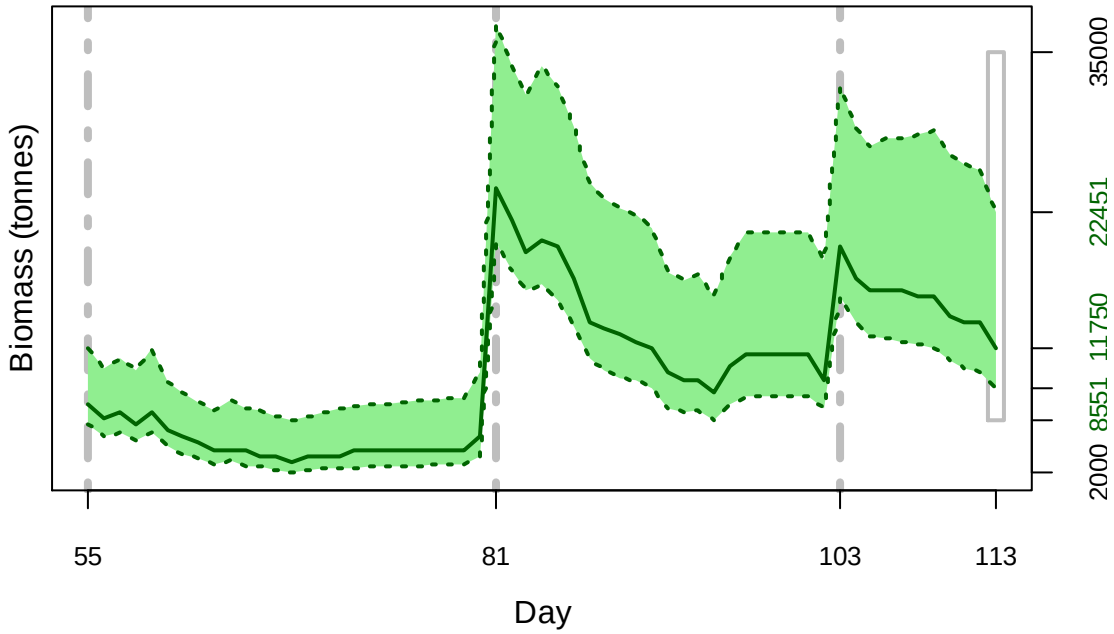

Figure 9. North sub-area. *Loligo* biomass time series estimated from Bayesian posterior of the depletion model ± 95% confidence intervals. Broken gray bars indicate days 55, 81, and 103, identified as the start of in-season depletions north. Note that the biomass 'footprint' on day 113 corresponds to the right-side plot of Figure 8.

At its highest point in the season (day 81; March 22nd, the start of the 2nd depletion period), estimated *Loligo* biomass north was 24,250 t ~ 95% CI [20,001 - 37,131] t (Figure 9).

South

In the south sub-area, the Bayesian posterior for catchability (q) (max. likelihood $q_S = 1.15 \times 10^{-3}$; Figure 10, left) was also closer to the pre-season prior ($_{prior}q_S = 1.32 \times 10^{-3}$; Figure 10, left, and equation **A3-S**) but proportionally less distant from the in-

season depletion ($_{depletion}$ q $_{S}$ = 0.55 × 10^{-3}; Figure 10, left, and **A5-S**). Bayesian optimization was weighted 0.592 for in-season depletion (**A4-S**) vs. 0.446 for the prior (**A8-S**); a comparatively small difference. Catch and effort time series in the south sub-area were characterized by the unusual situation that a new immigration was inferred from the sharp CPUE increase on day 81 (March 22nd), but then scarcely fished due to the even higher CPUE peak achieved in the north sub-area on the same day (Figure 6). As a result the estimation of biomass was relatively imprecise through much of the season time series (Figure 11).

The MCMC distribution of the posterior multiplied by average individual *Loligo* weight on the final day of the season (30.9 g; Figure A2-S), gave the likelihood distribution of *Loligo* final-day biomass shown in Figure 10, right, with maximum likelihood and 95% confidence interval of:

$$B_{S\ day\ 111} = 17{,}750\ t \sim 95\%\ CI\ [13{,}177 - 34{,}106]\ t \quad \textbf{(9)}$$

At its highest point in the season (day 92; April 2nd, the start of the 3rd depletion period), estimated *Loligo* biomass south was 43,750 t ~ 95% CI [33,936 - 77,355] t (Figure 11). Figure 11 also shows that the 4th depletion start on day 102 (April 12th) barely registers, suggesting that the CPUE peak identified on that day may have been a spurious occurrence from a single vessel (Figure 3).

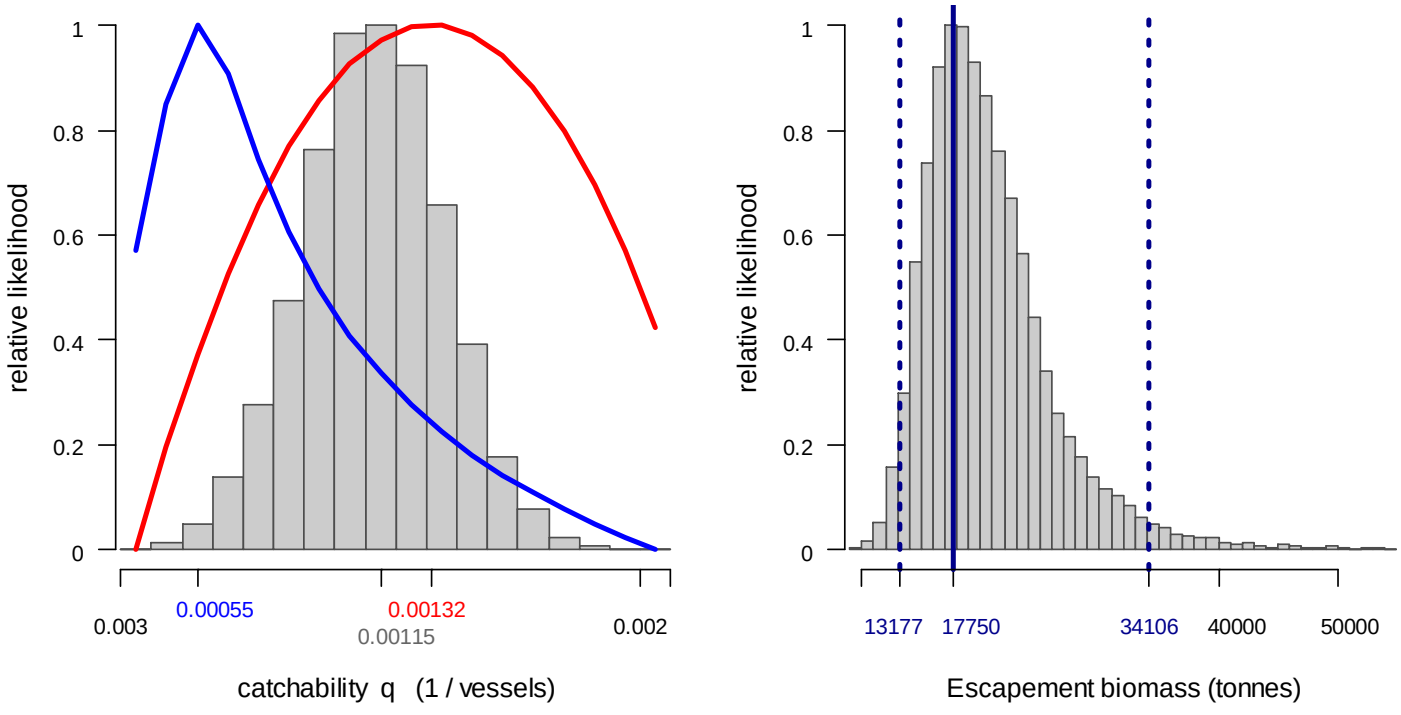

Figure 10. South sub-area. Left: Likelihood distributions for *Loligo* catchability. Red line: prior model (pre-season survey data), blue line: in-season depletion model, gray bars: combined Bayesian model. Right: Likelihood distribution (gray bars) of escapement biomass, from Bayesian posterior and average individual *Loligo* weight at the end of the season. Blue lines: maximum likelihood and 95% confidence interval. Note the correspondence to Fig. 11.

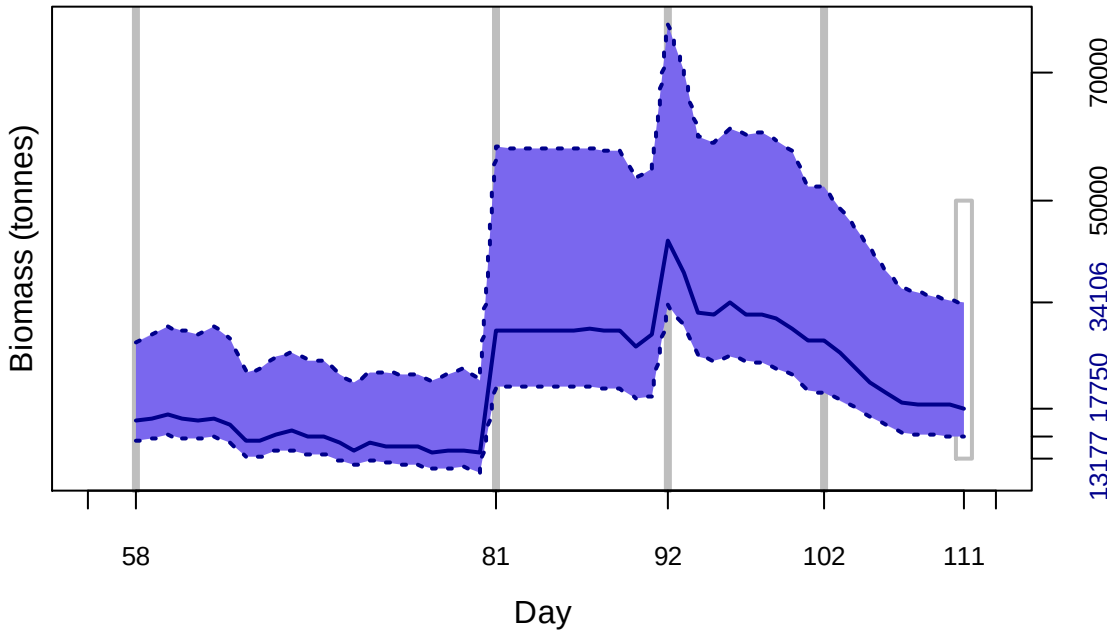

Figure 11. South sub-area. *Loligo* biomass time series estimated from Bayesian posterior of the depletion model ± 95% confidence intervals. Solid gray bars indicate days 58, 81, 92 and 102, identified as the start of in-season depletions south. Note that the biomass 'footprint' on day 111 corresponds to the right-side plot of Figure 10.

Escapement biomass

Total escapement biomass was defined as the aggregate biomass of *Loligo* at the end of the season (day 113; April 23rd) for north and south sub-areas combined (equations **8** and **9**). Because the south was only fished until day 111, estimated biomass south was adjusted by two additional days' natural mortality:

$$B_{S\ day\ 113} = B_{S\ day\ 111} \times e^{-M \times (113 - 111)}$$
$$= 17{,}283\ t \sim 95\%\ CI\ [12{,}830 - 33{,}209]\ t \quad \textbf{(10)}$$

The north and south sub-area biomasses are assumed to be independent and therefore the total was calculated by adding the respective north and south likelihood distributions in random order. The likelihood distribution of total escapement biomass is shown in Figure 12. Because both separate north and south escapement biomass distributions were right-skewed (Figures 8-right and 10-right), the maximum likelihood total escapement biomass is slightly higher than their sum:

$$B_{Total\ day\ 113} > B_{N\ day\ 113} + B_{S\ day\ 113}$$
$$= 30{,}500\ t \sim 95\%\ CI\ [24{,}059 - 49{,}207]\ t \quad \textbf{(11)}$$

The risk of the fishery, defined as the proportion of the total escapement biomass distribution below the conservation limit of 10,000 tonnes (Agnew et al., 2002; Barton, 2002), was calculated as effectively zero.

Figure 12 [next page]. Likelihood distribution with 95% confidence intervals of total *Loligo* escapement biomass at the end of the season (April 23rd).

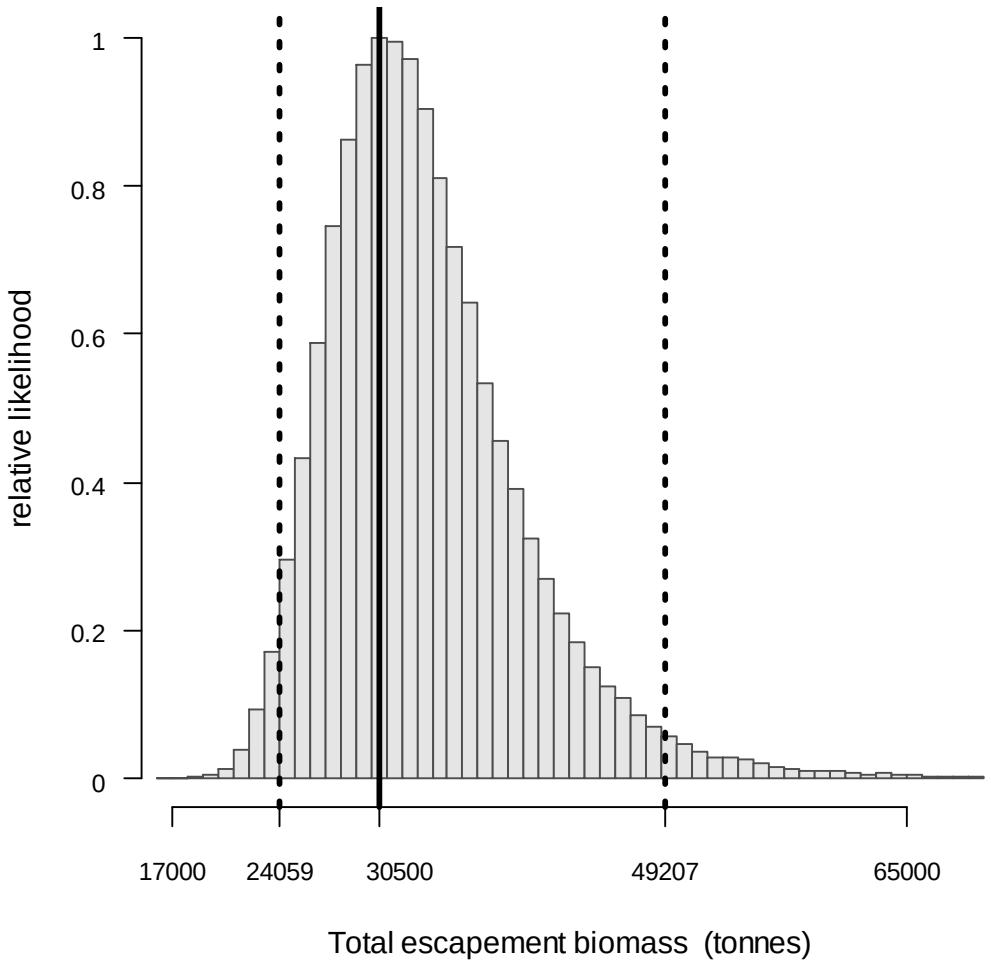

Immigration

Loligo immigration during the season was inferred as the difference between *Loligo* biomass at the end of the pre-season survey (Winter and Jürgens, 2014) and *Loligo* biomass at the end of the commercial season (escapement biomass) plus catch. The likelihood distribution of this difference was calculated by repeated iterations of drawing a random value from the escapement biomass distribution (equation **11**), adding the season catch, and subtracting a random draw from the likelihood distribution of the pre-season survey biomass:

$$
\begin{aligned}
B_{\text{Season Immigration}} &= B_{\text{Total day 113}} + C_{\text{Season}} - B_{\text{Survey end}} \\
&> 30{,}500\ [24{,}059 - 49{,}207] + 28{,}119 \\
&\quad - 34{,}673\ [22{,}182 - 47{,}762] \\
&= 26{,}750\ \text{t} \sim 95\%\ \text{CI}\ [10{,}398 - 46{,}512]\ \text{t} \qquad \textbf{(12)}
\end{aligned}
$$

Given the shape of distributions, the maximum likelihood outcome is again slightly higher than the sum of its maximum likelihood components. Note that $B_{\text{Season Immigration}}$ represents, more specifically, the biomass resulting from immigration rather than the biomass that immigrated; it does not taken into account that the squid would have been smaller on the date they entered the fishing zone and subsequently grown. However, in-season natural mortality is taken into account through the CNMD factor

(equation **6**). By this estimate, in-season immigration represents 46% of the *Loligo* biomass to have been present in the fishing zone in the 1st season of 2014: 26,750/(30,500 + 28,119) = 0.456.

Evaluation of season extension

During the one week of the season extended past previous years' scheduled end-date (April 15th to April 21st), >90% of effort was taken in the north sub-area, and the one vessel with observer coverage was in the north for 6 of the 7 days. Biological changes in *Loligo* catches were therefore examined for the north sub-area only.

Trends in sex proportions, maturity, and average individual *Loligo* weights were modelled vs. season day using generalized additive models (GAM). Trends were evaluated by the criterion that change is statistically significant to the extent that a horizontal line would intersect the 95% confidence intervals of the GAM plot (Swartzman et al., 1992). Average weight of males increased significantly from about day 93 (April 3rd) – well before the extension week – through the end of the season (Figure 13, top graph). Average weight of females increased significantly from about day 103 (April 13th, the start of the third immigration/depletion north) to day 107 (April 17th), then levelled to the end of the season (Figure 13, middle graph). The proportion of females showed a downward trend at the end of the season from day 105 (April 15th – the first extension day), although the decrease appeared to actually start on day 103 (Figure 13, bottom graph). However, this downward trend narrowly failed the criterion for statistical significance over the duration of the extension week. Average male maturity showed a continuously increasing trend over the duration of the season (Figure 14, top graph). Average female maturity did not show any statistically significant trend (Figure 14, bottom graph).

The only trend to (weakly) suggest an inflection coincident with the start of the season extension was thus the decrease in female proportion, consistent with the report by Arkhipkin and Middleton (2002) that ontogenetic migrations are undertaken by females earlier into deeper water. Other trends followed biological expectations: *Loligo* squid naturally increase in weight and maturity as they grow. The generally low significance of these trends associated with the season extension may be partly due (besides the relatively short duration of the extension) to overlap of the two annual cohorts in- and out-migrating through the fishing zone at this time of year (Hatfield, 1996; Agnew et al., 1998).

The season extension comprised 11.9% of the total commercial season effort (104 vessel-days) and 13.6% of the *Loligo* catch (3823 t; both percentages calculated with inclusion of the two-day offset for the late-starting vessel). Ignoring the small bias that vessels typically fish harder on the last day, these results indicate that the period of season extension yielded better-than-average fishing. Notably, in-season immigrations occurred just one day in the north and two days in the south before what would previously have been the last day of the season (April 14th). With no evidence of strong biological impacts, and an escapement biomass well above the conservation threshold, it may be concluded that implementation of the one-week extension was appropriate for this season.

Figure 13 [below]. GAM plots ± 95% confidence intervals of - Top graph: average male weight (kg), middle graph: average female weight (kg), bottom graph: proportion of females;

from observer samples in the north sub-area. Note correspondence of the plot symbols with respective graphs in Figure 7. Broken gray bar indicates day 103, identified as the start of the third in-season depletion north. Dotted gray bars indicate the start and end of the one-week season extension, days 105 to 113, which is also under-shaded gray.

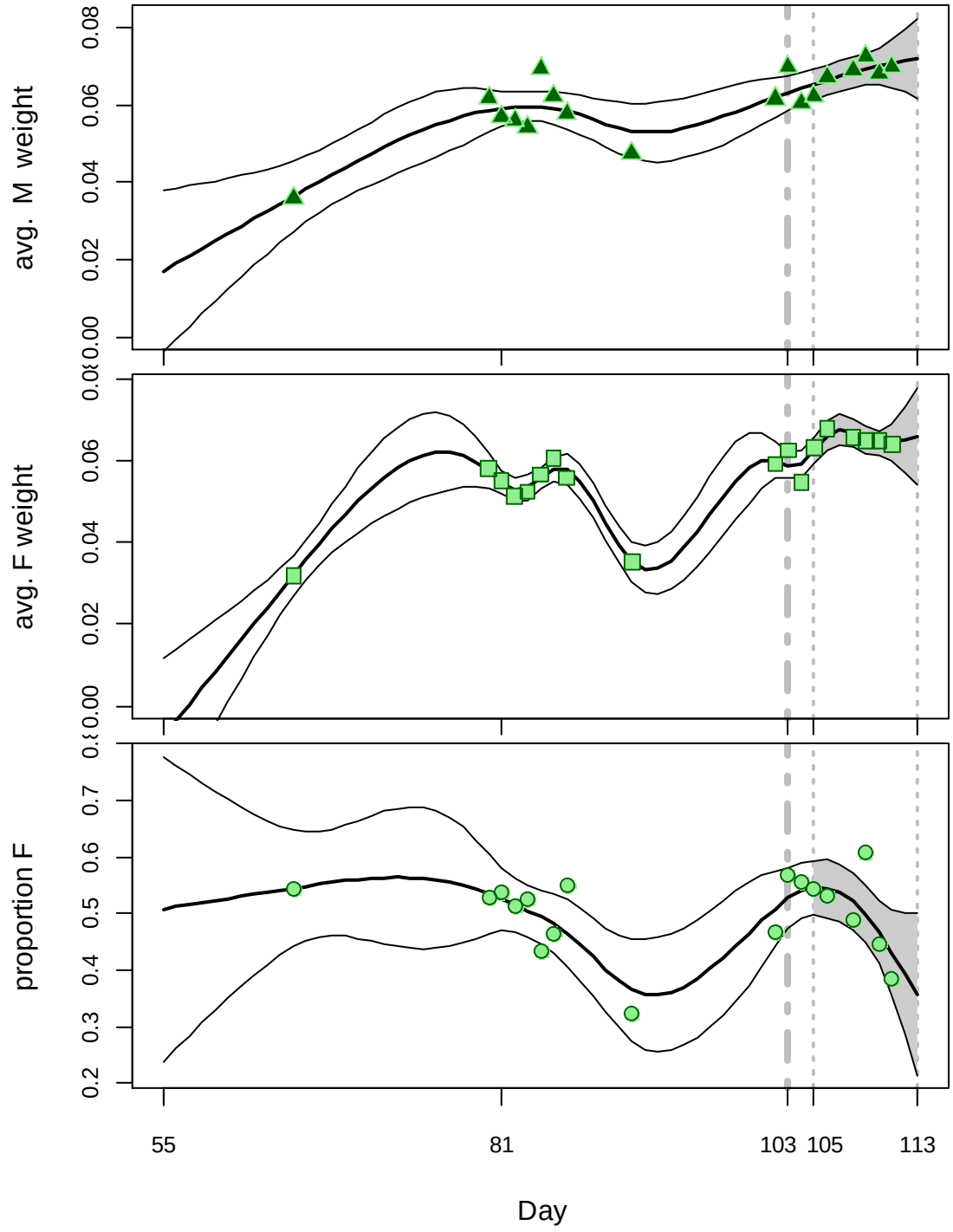

Figure 14 [next page]. GAM plots ± 95% confidence intervals of - Top graph: average male maturity, bottom graph: average female maturity; from observer samples in the north sub-area. Note correspondence of the plot symbols with respective graphs in Figure 7. Other graph notations as in Figure 13.

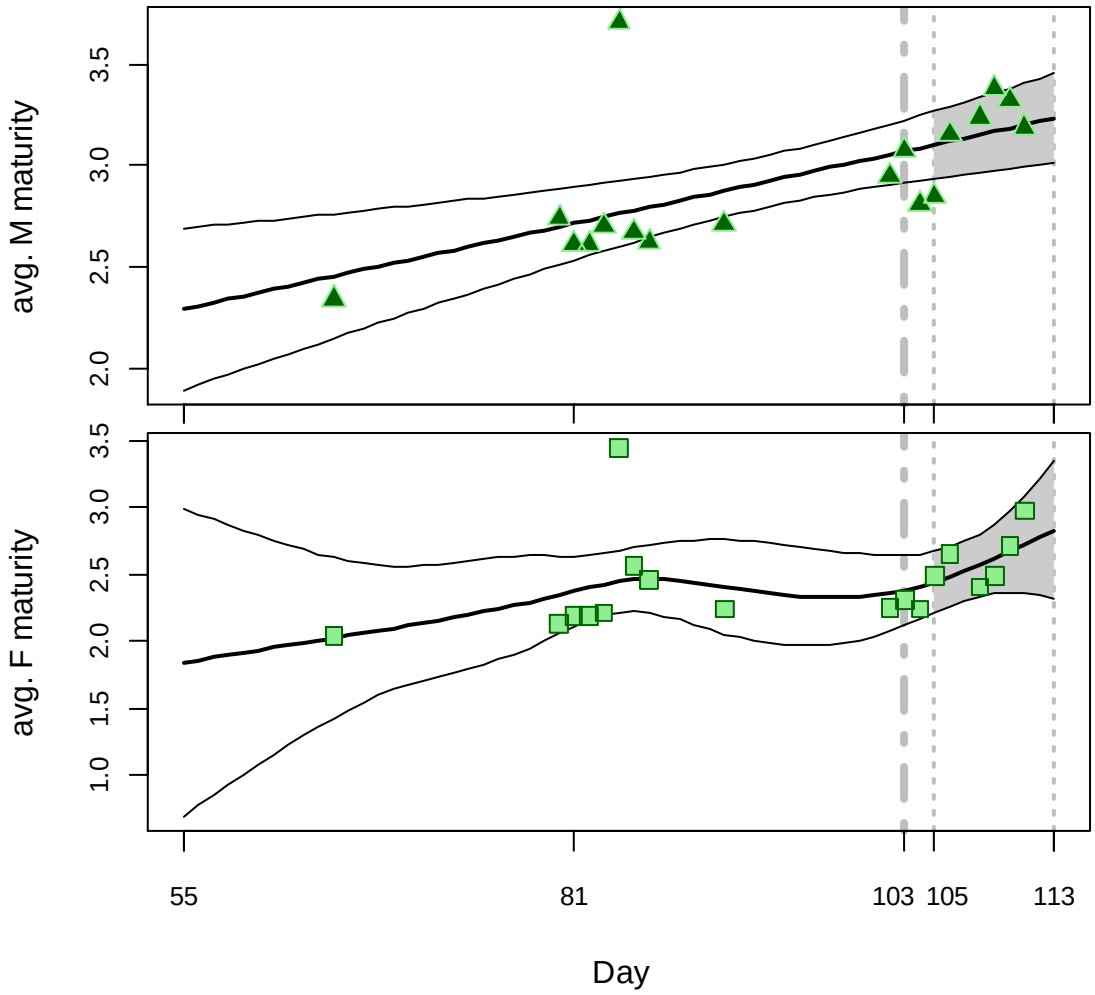

References

Agnew, D.J., Baranowski, R., Beddington, J.R., des Clers, S., Nolan, C.P. 1998. Approaches to assessing stocks of *Loligo gahi* around the Falkland Islands. Fisheries Research 35:155-169.

Agnew, D. J., Beddington, J. R., and Hill, S. 2002. The potential use of environmental information to manage squid stocks. Canadian Journal of Fisheries and Aquatic Sciences, 59: 1851–1857.

Arkhipkin, A.I., Hatfield, E.M.C., Rodhouse, P.G.K. 2013. Chapter V. *Doryteuthis gahi*, Patagonian Long-Finned Squid. In: Rosa, R., O'Dor, R., Pierce, G.J. (Eds.), Advances in squid biology, ecology and fisheries, Part I – Myopsid squids. Nova Science Publishers, Inc., New York, pp. 123-157.

Arkhipkin, A.I., Middleton, D.A.J. 2002. Sexual selection in ontogenetic migrations by the squid *Loligo gahi* around the Falkland Islands. Bulletin of Marine Science 71: 109-127.

Arkhipkin, A.I., Middleton, D.A.J., Barton, J. 2008. Management and conservation of a short-lived fishery resource: *Loligo gahi* around the Falkland Islands. American Fisheries Society Symposium 49:1243-1252.

Barton, J. 2002. Fisheries and fisheries management in Falkland Islands Conservation Zones. Aquatic Conservation: Marine and Freshwater Ecosystems, 12: 127–135.

Brooks, S.P., Gelman, A. 1998. General methods for monitoring convergence of iterative simulations. Journal of computational and graphical statistics 7:434-455.

Brotz, L., Cheung, W.W.L., Kleisner, K., Pakhomov, E., Pauly, D. 2012. Increasing jellyfish populations: trends in Large Marine Ecosystems. Hydrobiologia 690: 3-20.

DeLury, D.B. 1947. On the estimation of biological populations. Biometrics 3:145-167.

Fisheries Committee. 2013. Re-allocation of fishing effort between 1st and 2nd *Loligo* seasons. Proposal to the Fisheries Committee, December 2013. 4 p.

Gamerman, D., Lopes, H.F. 2006. Markov Chain Monte Carlo. Stochastic simulation for Bayesian inference. 2nd edition. Chapman & Hall/CRC.

Hatfield, E.M.C. 1996. Towards resolving multiple recruitment into loliginid fisheries: *Loligo gahi* in the Falkland Islands fishery. ICES Journal of Marine Science 53: 565-575.

Jones, J. 2014a. Observer Report 988. Technical Document, FIG Fisheries Department. 30 p.

Jones, J. 2014b. Observer Report 995. Technical Document, FIG Fisheries Department. 20 p.

Lee, B. 2014. Observer Report 992. Technical Document, FIG Fisheries Department. 18 p.

Magnusson, A., Punt, A., Hilborn, R. 2013. Measuring uncertainty in fisheries stock assessment: the delta method, bootstrap, and MCMC. Fish and Fisheries 14: 325-342.

Nash, J.C., Varadhan, R. 2011. optimx: A replacement and extension of the optim() function. R package version 2011-2.27. http://CRAN.R-project.org/package=optimx

Patterson, K.R. 1988. Life history of Patagonian squid *Loligo gahi* and growth parameter estimates using least-squares fits to linear and von Bertalanffy models. Marine Ecology Progress Series 47:65-74.

Payá, I. 2010. Fishery Report. *Loligo gahi*, Second Season 2009. Fishery statistics, biological trends, stock assessment and risk analysis. Technical Document, Falkland Islands Fisheries Department. 54 p.

Punt, A.E., Hilborn, R. 1997. Fisheries stock assessment and decision analysis: the Bayesian approach. Reviews in Fish Biology and Fisheries 7:35-63.

Roa-Ureta, R. 2012. Modelling in-season pulses of recruitment and hyperstability-hyperdepletion in the *Loligo gahi* fishery around the Falkland Islands with generalized depletion models. ICES Journal of Marine Science 69: 1403–1415.

Roa-Ureta, R., Arkhipkin, A.I. 2007. Short-term stock assessment of *Loligo gahi* at the Falkland Islands: sequential use of stochastic biomass projection and stock depletion models. ICES Journal of Marine Science 64:3-17.

Rosenberg, A.A., Kirkwood, G.P., Crombie, J.A., Beddington, J.R. 1990. The assessment of stocks of annual squid species. Fisheries Research 8:335-350.

Swartzman, G., Huang, C., Kaluzny, S. 1992. Spatial analysis of Bering Sea groundfish survey data using generalized additive models. Canadian Journal of Fisheries and Aquatic Sciences 49: 1366-1378.

Winter, A., Arkhipkin, A. 2012. Predicting recruitment pulses of Patagonian squid in the Falkland Islands fishery. World Fisheries Congress, Edinburgh, Scotland.

Winter, A., Jürgens, L. 2014. *Loligo* stock assessment survey, 1st season 2014. Technical Document, Falkland Islands Fisheries Department. 18 p.

Zhang, H.-M., Bates, J.J., Reynolds, R.W. 2006. Assessment of composite global sampling: Sea surface wind speed. Geophysical Research Letters, 33: L17714.

Appendix

Prior estimates and CV

The pre-season survey (Winter and Jürgens, 2014) had estimated *Loligo* biomasses of 13,096 t (standard deviation: ± 4,155 t) north of 52º S and 21,577 t (standard deviation: ± 5,033 t) south of 52º S. From modelled survey catchability, Payá (2010) estimated a net escapement of up to 22%, which was added to the standard deviation:

$$13{,}096 \pm \left(\frac{4{,}155}{13{,}096} + .22 \right) \;=\; 13{,}096 \pm 53.7\% \;=\; 13{,}096 \pm 7{,}036 \text{ t.} \qquad \textbf{(A1-N)}$$

$$21{,}577 \pm \left(\frac{5{,}033}{21{,}577} + .22 \right) \;=\; 21{,}577 \pm 45.3\% \;=\; 21{,}577 \pm 9{,}780 \text{ t.} \qquad \textbf{(A1-S)}$$

The 22% was added as a linear increase in the variability, but was not used to reduce the total estimate, because *Loligo* that escape one trawl are likely to be part of the biomass concentration that is available to the next trawl. This estimate in biomass was converted to an estimate in numbers using the size-frequency distributions sampled during the pre-season survey (Winter and Jürgens, 2014).

Loligo were sampled at 59 pre-season survey stations, giving average mantle lengths (both sexes; weighted for *Loligo* density distribution) of 11.88 cm north and 11.29 cm south, corresponding to respectively 0.045 and 0.040 kg average individual weight. Variability distributions of average individual weight were estimated by randomly re-sampling the length-frequency data 10,000×, giving coefficients of variation 0.82% north and 0.72% south. Average coefficients of variation of the length-weight relationship (equation **7**) were 7.28% north and 7.27% south. Combining all sources of variation with the pre-season survey biomass estimates and average individual weights gave estimated *Loligo* numbers at season start (February 24th; day 55) of:

$$_{\text{prior}}N_{\text{N day 55}} \;=\; \frac{13{,}096 \times 1000}{0.045} \pm \sqrt{53.7\%^2 + 0.82\%^2 + 7.28\%^2}$$

$$= 0.292 \times 10^9 \pm 54.2\% \;=\; 0.292 \times 10^9 \pm 0.158 \times 10^9 \qquad \textbf{(A2-N)}$$

$$_{\text{prior}}N_{\text{S day 55}} \;=\; \frac{21{,}577 \times 1000}{0.040} \pm \sqrt{45.3\%^2 + 0.72\%^2 + 7.27\%^2}$$

$$= 0.539 \times 10^9 \pm 45.9\% \;=\; 0.539 \times 10^9 \pm 0.248 \times 10^9 \qquad \textbf{(A2-S)}$$

On day 55 seven vessels were fishing *Loligo* in the north and eight vessels in the south; a good representation in both sub-areas. Therefore the fishery on day 55 was taken directly to calculate the catchability coefficient (q) priors:

$$_{\text{prior}}q_{\text{N}} = C(N)_{\text{N day 55}} / (_{\text{prior}}N_{\text{N day 55}} \times E_{\text{N day 55}})$$
$$= (C(B)_{\text{N day 55}} / Wt_{\text{N day 55}}) / (_{\text{prior}}N_{\text{N day 55}} \times E_{\text{N day 55}})$$
$$= (203.7 \text{ t} / 0.035 \text{ kg}) / (0.292 \times 10^9 \times 7 \text{ vessel-days})$$

$$= 2.836 \times 10^{-3} \text{ vessels}^{-1} \quad \textbf{(A3-N)}$$

$$\begin{aligned} {}_{\text{prior}}q_{S} &= C(N)_{S\ \text{day}\ 55} / ({}_{\text{prior}}N_{S\ \text{day}\ 55} \times E_{S\ \text{day}\ 55}) \\ &= (C(B)_{S\ \text{day}\ 55} / Wt_{S\ \text{day}\ 55}) / ({}_{\text{prior}}N_{S\ \text{day}\ 55} \times E_{S\ \text{day}\ 55}) \\ &= (238.5\ \text{t} / 0.042\ \text{kg}) / (0.539 \times 10^{9} \times 8\ \text{vessel-days}) \\ &= 1.316 \times 10^{-3}\ \text{vessels}^{-1} \quad \textbf{(A3-S)} \end{aligned}$$

CVs of the priors were calculated as the sums of variability in ${}_{\text{prior}}N$ (equations **A2**) plus variability in the catches of vessels on the start day (day 55):

$$CV_{\text{prior N}} = \sqrt{54.2\%^{2} + \left(\frac{SD\left(C(B)_{\text{N vessels day 55}}\right)}{\text{mean}\left(C(B)_{\text{N vessels day 55}}\right)} \right)^{2}}$$

$$= \sqrt{54.2\%^{2} + 13.0\%^{2}} = 55.8\% \quad \textbf{(A4-N)}$$

$$CV_{\text{prior S}} = \sqrt{45.9\%^{2} + \left(\frac{SD\left(C(B)_{\text{S vessels day 55}}\right)}{\text{mean}\left(C(B)_{\text{S vessels day 55}}\right)} \right)^{2}}$$

$$= \sqrt{45.9\%^{2} + 37.3\%^{2}} = 59.2\% \quad \textbf{(A4-S)}$$

Depletion model estimates and CV

For the north sub-area, the equivalent of equation **2** with three N_{day} was optimized on the difference between predicted catches and actual catches (equation **3**), resulting in parameters values:

$${}_{\text{depletion}}N1_{\text{N day 55}} = 0.149 \times 10^{9}; \qquad {}_{\text{depletion}}N2_{\text{N day 81}} = 0.318 \times 10^{9}$$

$${}_{\text{depletion}}N3_{\text{N day 103}} = 0.200 \times 10^{9}$$

$${}_{\text{depletion}}q_{N} = 4.751 \times 10^{-3}\ \text{vessels}^{-1} \quad \textbf{(A5-N)}$$

These parameters produced the fit between predicted and actual catches shown in Figure A1-N.

The root-mean-square deviation of predicted vs. actual catches was calculated and divided by the mean actual catch to give:

$$CV_{\text{rmsd N}} = \frac{\sqrt{\sum_{i}\left({}_{\text{predicted}}C(N)_{\text{N day i}} - {}_{\text{actual}}C(N)_{\text{N day i}}\right)^{2}}}{\text{mean}\left({}_{\text{actual}}C(N)_{\text{N day i}}\right)}$$

$$= 2.209 \times 10^{6} / 8.122 \times 10^{6} = 27.2\% \quad \textbf{(A6-N)}$$

$CV_{\text{rmsd N}}$ was added to the variability in depletion optimization inferred from variability in the daily average individual *Loligo* weights. In previous assessments,

variability in daily average individual *Loligo* weights was included as a randomized multiplicative factor of the MCMC distribution of *Loligo* numbers, to estimate biomass variability. However, *Loligo* numbers are derived in part from *Loligo* weights rather than being statistically independent, and therefore a truer measure of biomass variability may be obtained by estimating the effect of weight variation in the original depletion optimization.

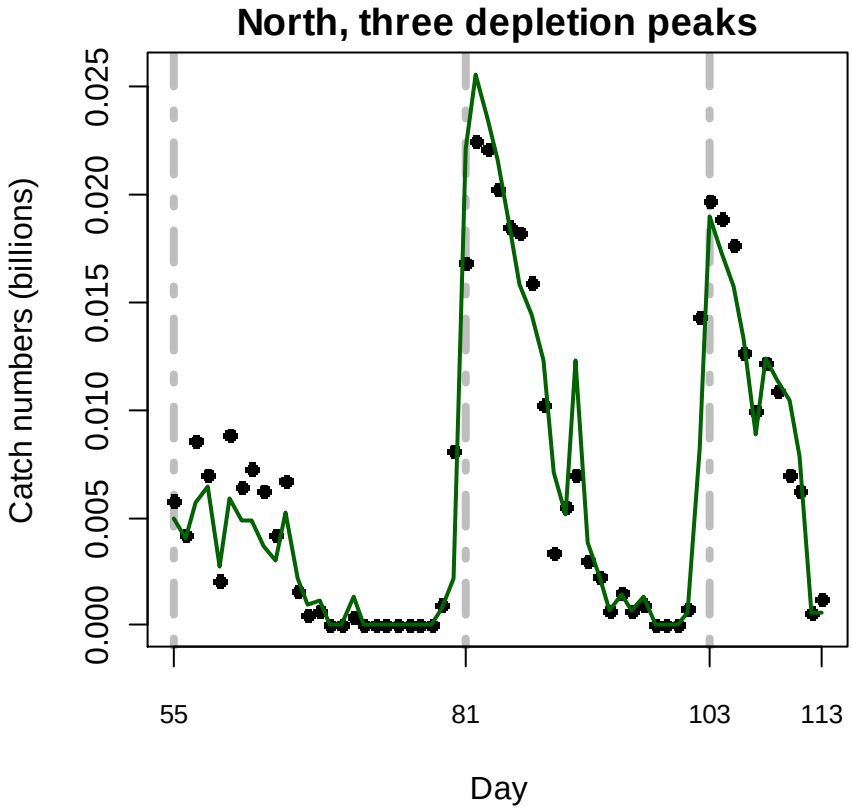

Figure A1-N. Daily catch numbers estimated from actual catch (black points) and predicted from the depletion model (green line) in the north sub-area.

Figure A2-N shows the season time series of individual *Loligo* weights in the north sub-area. A generalized additive model (GAM) was calculated for the daily average individual *Loligo* weight trend. Random permutation of residual differences between GAM-predicted vs. recorded daily average individual weights was used to create re-samples of estimated catch numbers per day ($C(N)_{day} = C(B)_{day} / {}_{avg}Wt_{day}$), which were then entered in the depletion optimization. This process was iterated 1000×. The optimized q value was retained from each iteration and the variability of the optimization with respect to average individual weight calculated as:

$$CV_{optim\ Wt\ N} = \frac{sd\left(q_{perm\ N}\right)}{mean\left(q_{perm\ N}\right)} = 5.6\% \qquad \textbf{(A7-N)}$$

CVs of the depletion were then calculated as the sum:

$$CV_{depletion\ N} = \sqrt{CV_{rmsd\ N}{}^2 + CV_{optim\ Wt\ N}{}^2} = \sqrt{27.2\%^2 + 5.6\%^2}$$

$$= \quad 27.8\% \qquad \textbf{(A8-N)}$$

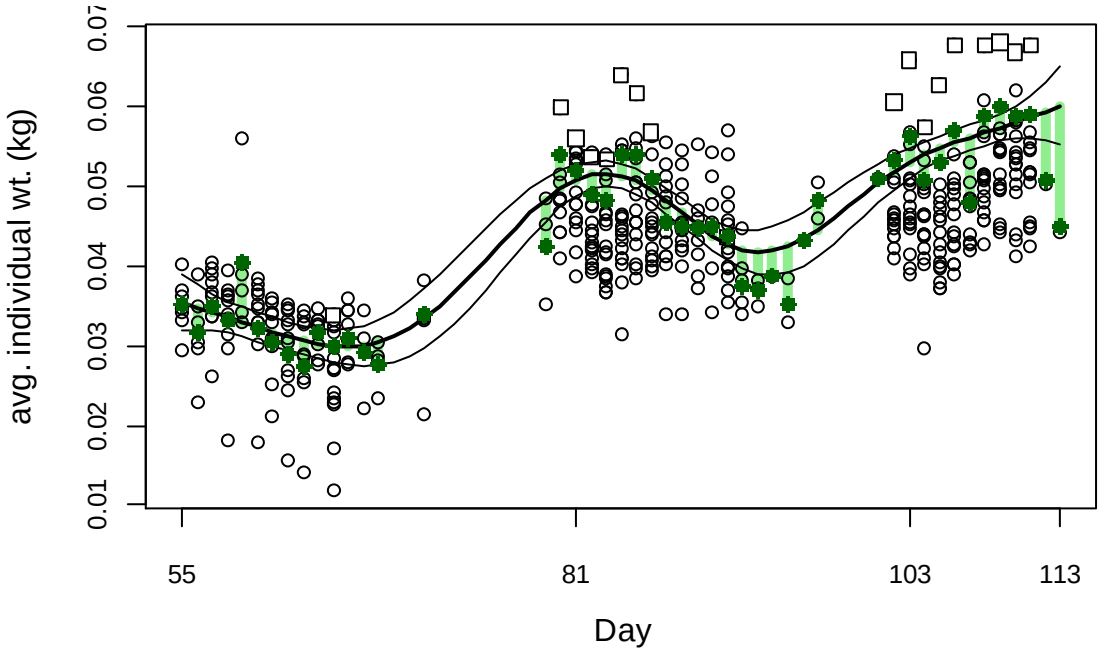

Figure A2-N. North sub-area daily average individual *Loligo* weights from commercial size categories per vessel (circles), observer measurements (squares), combined daily averages (green circles), GAM of the daily trend ± 95% conf. int. (black lines), and residual differences between the combined daily averages and GAM (light green bars).

For the south sub-area, the equivalent of equation **2** with four N_{day} was optimized on the difference between predicted catches and actual catches (equation **3**), resulting in parameters values:

$$_{depletion}N1_{S\ day\ 58} = 0.961 \times 10^{9}; \qquad _{depletion}N2_{S\ day\ 81} = 0.887 \times 10^{9}$$

$$_{depletion}N3_{S\ day\ 92} = 0.530 \times 10^{9}; \qquad _{depletion}N4_{S\ day\ 102} = 0.000 \times 10^{9}$$

$$_{depletion}q_{S} = 0.555 \times 10^{-3}\ \text{vessels}^{-1} \qquad \textbf{(A5-S)}$$

These parameters produced the fit between predicted and actual catches shown in Figure A1-S.

The root-mean-square deviation of predicted vs. actual catches was calculated, and its CV assigned to the depletion model q parameter:

$$CV_{rmsd\ S} = \frac{\sqrt{\sum_{i}\left(_{predicted}C(N)_{S\ day\ i} - _{actual}C(N)_{S\ day\ i}\right)^{2}}}{\text{mean}\left(_{actual}C(N)_{S\ day\ i}\right)}$$

$$= 1.290 \times 10^{6} / 6.355 \times 10^{6} = 20.3\% \qquad \textbf{(A6-S)}$$

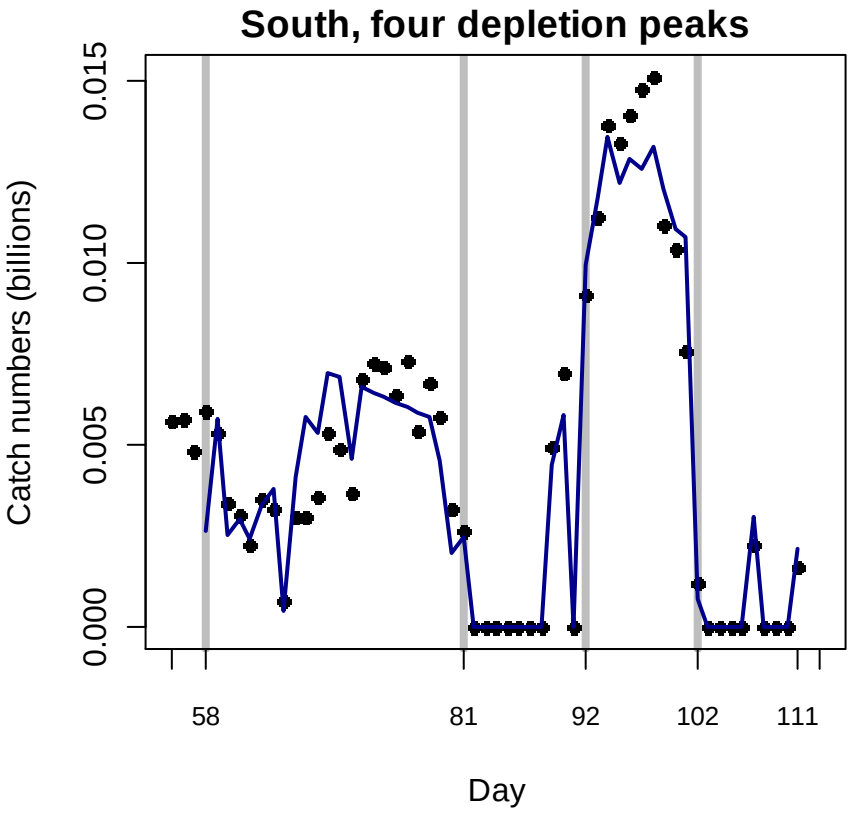

Figure A1-S. Daily catch numbers estimated from actual catch (black points) and predicted from the depletion model (blue line) in the south sub-area.

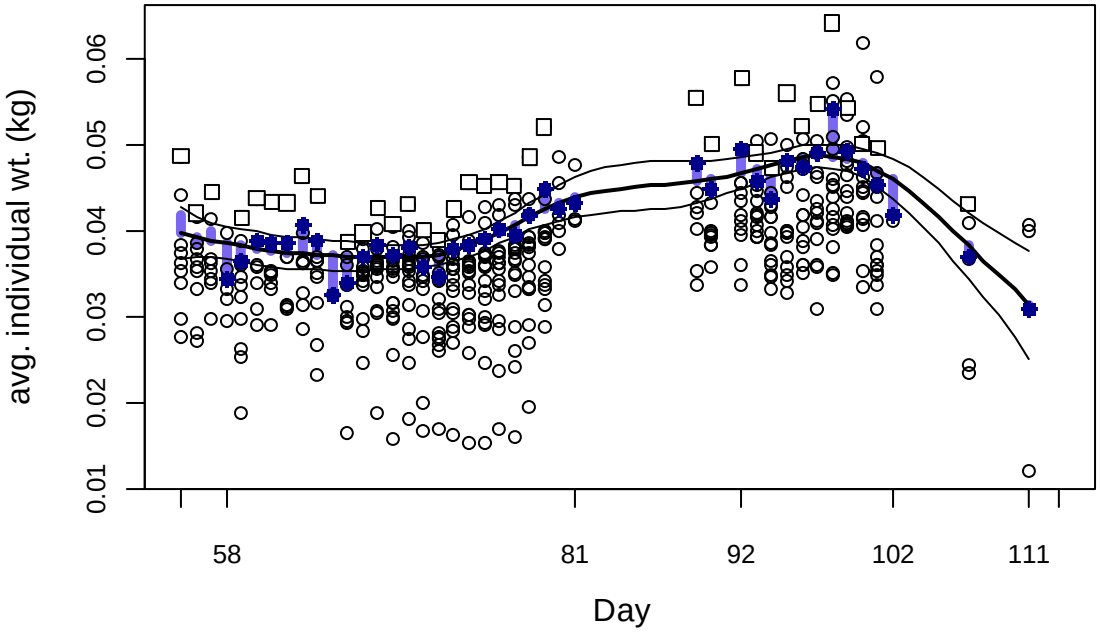

Figure A2-S. South sub-area daily average individual *Loligo* weights from commercial size categories per vessel (circles), observer measurements (squares), combined daily averages (blue circles), GAM of the daily trend ± 95% conf. int. (black lines), and residual differences between the combined daily averages and GAM (light blue bars).

$CV_{rmsd\ S}$ was added to the variability in depletion optimization inferred from variability in the daily average individual *Loligo* weights (Figure A2-S):

$$CV_{optim\ Wt\ S} = \frac{sd\left(q_{perm\ S}\right)}{mean\left(q_{perm\ S}\right)} = 39.7\% \quad \textbf{(A7-S)}$$

CVs of the depletion were then calculated as the sum:

$$CV_{depletion\ S} = \sqrt{CV_{rmsd\ S}^{\ 2} + CV_{optim\ Wt\ S}^{\ 2}} = \sqrt{20.3\%^2 + 39.7\%^2}$$
$$= 44.6\% \quad \textbf{(A8-S)}$$

Sea wind patterns

Figure A3 [below]. Sea wind vectors at 0.25° resolution, from blended satellite observations (Zhang et al., 2006), over the eight-day period spanning the exceptionally high *Loligo* catch rates in the north sub-area.

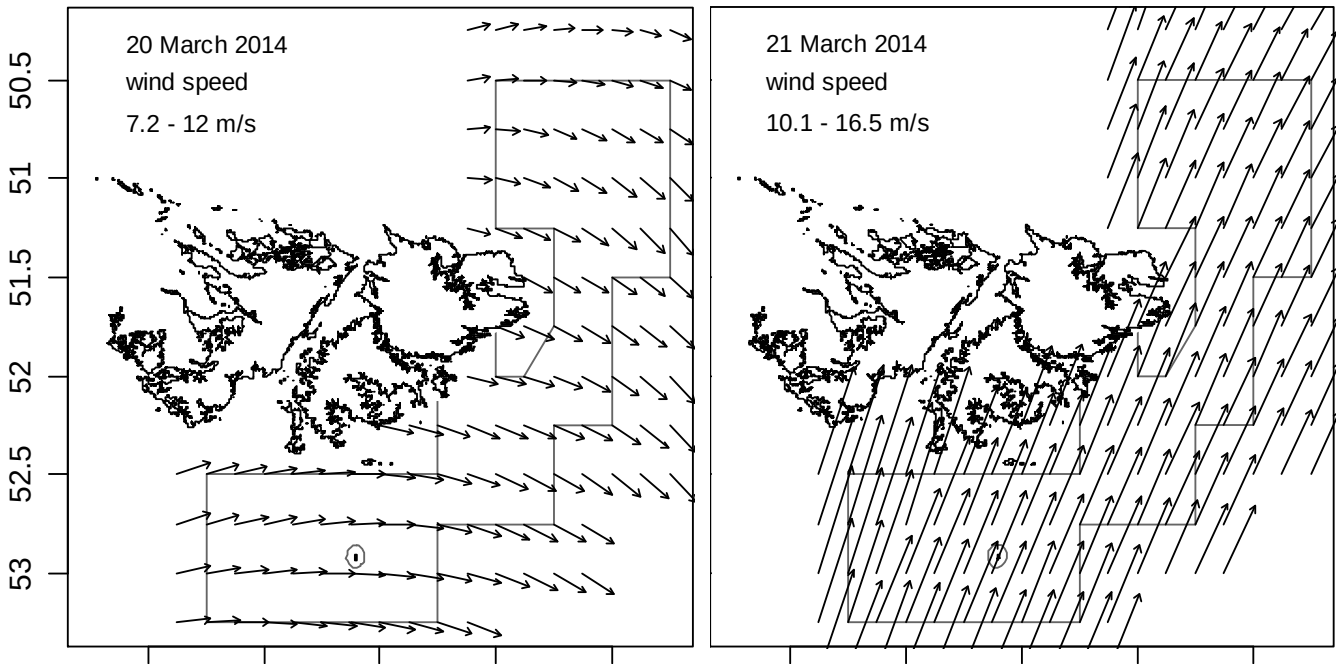

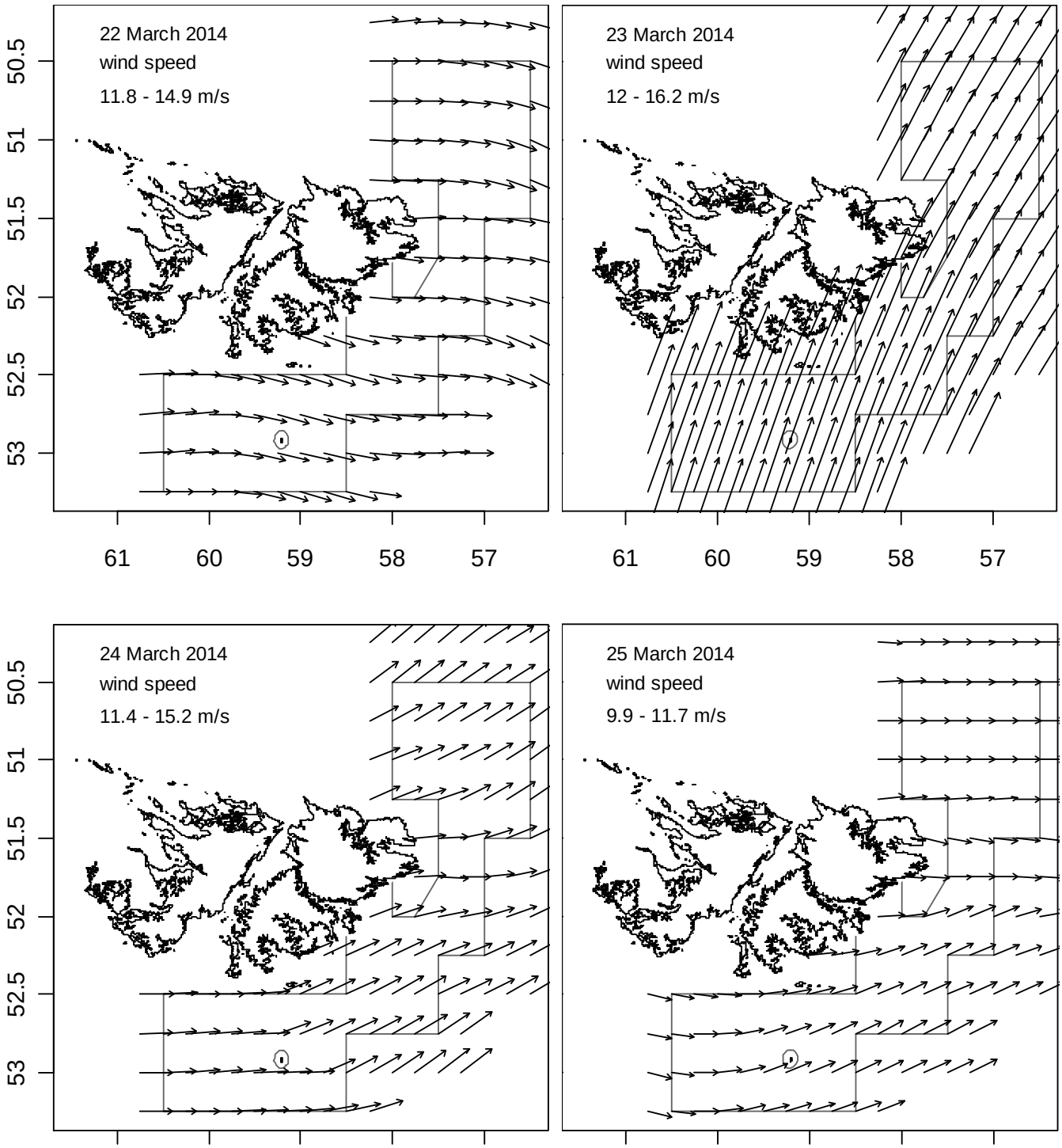
22 March 2014
wind speed
11.8 - 14.9 m/s
23 March 2014
wind speed
12 - 16.2 m/s
24 March 2014
wind speed
11.4 - 15.2 m/s
25 March 2014
wind speed
9.9 - 11.7 m/s
50.5
51
51.5
52
52.5
53
61
60
59
58
57

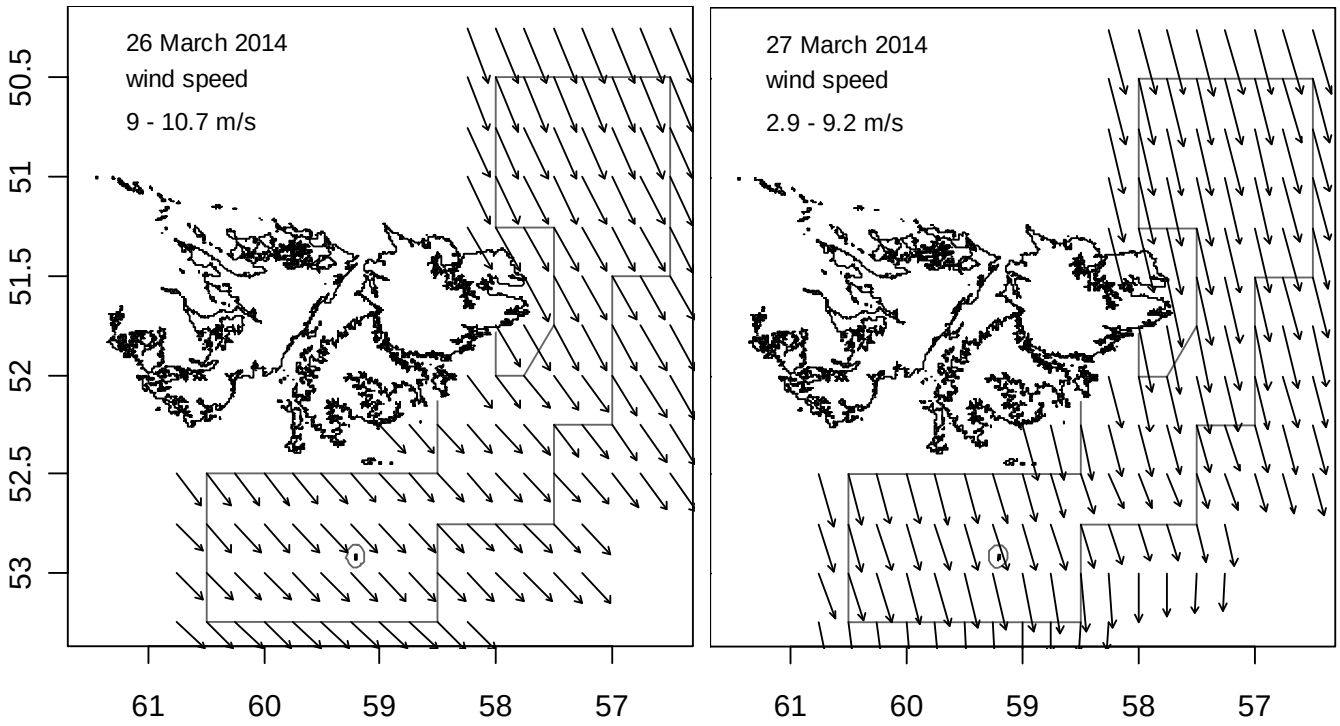
26 March 2014
wind speed
9 - 10.7 m/s
27 March 2014
wind speed
2.9 - 9.2 m/s
50.5
51
51.5
52
52.5
53
61
60
59
58
57